

# Aggregation of dinuclear {Fe<sub>2</sub>hpdta} units to form polynuclear oxy/hydroxy-bridged Fe(III) coordination complexes†

Wolfgang Schmitt,<sup>\*a</sup> Lei Zhang,<sup>a</sup> Christopher E. Anson<sup>b</sup> and Annie K. Powell<sup>\*b</sup>

Received 13th June 2010, Accepted 13th August 2010

DOI: 10.1039/c0dt00655f

An approach for the preparation of oxy/hydroxy bridged Fe<sup>III</sup> clusters that takes advantage of hydrolytic condensations of well defined {Fe<sub>2</sub>hpdta(H<sub>2</sub>O)<sub>4</sub>} building units is presented. Co-ligands such as tripodal H<sub>3</sub>tea or bidentate organic bases such as ethylenediamine (enH<sub>2</sub>) can be used to complete the coordination spheres of the Fe<sup>III</sup> centres and stabilise unsymmetrical iron-oxo clusters with non-zero magnetic ground spin-states. This strategy led to the isolation of a pentanuclear complex [Fe<sub>5</sub>(μ<sub>3</sub>-O)(hpdta)(H<sub>3</sub>tea)(Htea)<sub>2</sub>(tea)]·{N(C<sub>2</sub>H<sub>4</sub>OH)<sub>3</sub>}·2EtOH·7H<sub>2</sub>O (**1**) and a nonanuclear coordination complex [Fe<sub>9</sub>(μ<sub>3</sub>-O)<sub>5</sub>(μ-OH)<sub>5</sub>(en)<sub>6</sub>(hpdta)<sub>2</sub>](NO<sub>3</sub>)<sub>2</sub>·7H<sub>2</sub>O (**2**).

## 1 Introduction

Coordination clusters are characterised by their zero-dimensionality and associated topology and are attracting an ever increasing scientific interest as a result of the possibility of observing quantum behaviour in terms of their magnetic and electronic properties. These molecular-based systems can range from relatively small oligonuclear complexes such as triangular arrangements of metal ions through much larger nanosized oxo-bridged clusters leading to infinite solid-state structures displaying cooperative magnetic properties.<sup>1</sup> In the nanosized zero dimensional regime, cooperatively coupled ions in coordination clusters can result in superparamagnetic properties, which, when combined with quantum behaviour, might find uses in future technological applications for information storage and quantum devices.<sup>2</sup> In addition to their interesting magnetic properties, polynuclear Fe<sup>III</sup>-oxo-clusters provide insights into the biochemistry and geochemistry of iron, in particular in aqueous media where such aggregates form easily and can give insights into nucleation and growth of iron oxyhydroxide minerals.<sup>3</sup> Thus, these compounds serve as a distinct class of model compounds for physico- and bio-chemical studies and chemists have applied a variety of synthetic methodologies to produce new examples of these nanosized, magnetic molecules.<sup>4,5</sup> A goal of such synthetic programmes is to develop means to rationalise the aggregation processes occurring in solution by combining molecular sub-units in a predictable way to produce the desired complexes. However, for most transition metal systems such a high degree of control is still rather in the realm of wishful thinking than in that of reality. In particular for Fe<sup>III</sup> chemistry in hydrolysing aqueous environments, the overwhelming tendency of hydrolytic processes to reach the thermodynamic sink of amorphous Fe<sup>III</sup> hydroxides must be brought under control.

<sup>a</sup>School of Chemistry & Centre for Research on Adaptive Nanostructures and Nanodevices (CRANN), University of Dublin, Trinity College, Dublin 2, Ireland. E-mail: schmittw@tcd.ie; Fax: +353 1 671 2826; Tel: +353 1 896 3495

<sup>b</sup>Institute of Inorganic Chemistry, Karlsruhe Institute of Technology, Engesserstr. 15, 76131, Karlsruhe, Germany. E-mail: powell@kit.edu; Fax: +49 721-608-8142

† CCDC reference numbers 781103 (**1**) and 781104 (**2**). For crystallographic data in CIF or other electronic format see DOI: 10.1039/c0dt00655f

Biological systems which have adapted to deal with the prevailing oxidising nature of the Earth's atmosphere serve as a special inspiration to synthesising tailored systems involving iron-oxygen aggregates. Iron is found in nearly all living organisms bound to a diverse array of proteins and enzymes and since its biochemistry is controlled to a large extent by coordination chemistry principles, biochemical and biomineralisation processes can serve as paradigms for the synthesis of oxo-clusters.<sup>6</sup>

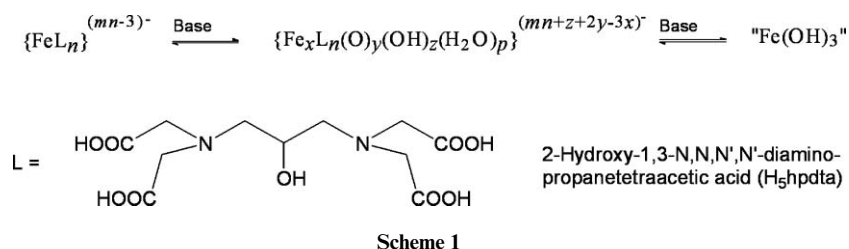
Thus, we have taken inspiration from the versatility of biological systems to control the structure and supramolecular arrangements of polynuclear oxo/hydroxo bridged Fe<sup>III</sup> species and have explored ways of preparing materials using the natural hydrolysis of metal ions as a basic chemical driving force.<sup>7</sup> Hydrolysis is the result of the activation of ligated waters by the metal ion. These water molecules can lose protons easily and tend to react in ololation and oxolation processes to form hydroxide and oxide bridges between metal centres.

Previously, we have shown how chelating ligands based on the functionalities found in amino acids can be used to control the hydrolysis reactions of Fe<sup>III</sup> ions and allow various cluster-based magnetic materials or coordination networks to be isolated and characterised.<sup>8</sup> Often, less protic reaction solutions containing specific amounts or just traces of water can offer an increased control over the hydrolytic condensation which usually occurs irreversibly in purely aqueous systems on a millisecond timescale.<sup>3</sup> Here we report on the results we obtain applying these principles using the ligands H<sub>3</sub>hpdta (Scheme 1), triethanolamine (H<sub>3</sub>tea) and ethylenediamine (enH<sub>2</sub>).

## 2 Results and discussion

### 2.1 Synthetic approach to produce polynuclear oxo-hydroxo bridged Fe<sup>III</sup>/hpdta complexes

In the H<sub>3</sub>hpdta reaction system the activation of coordinated water ligands is of importance in rationalising the approach to creating larger aggregates. We have previously reported<sup>7,8</sup> the homologous build-up of oxo/hydroxo-clusters by linking dinuclear {Fe<sub>2</sub>(hpdta)} building units *via* condensation reactions resulting in tetranuclear and hexanuclear oxo clusters. In addition to these intermolecular condensation reactions, pH changes also



effect intramolecular interactions, for instance, core rearrangement reactions where the dinuclear subunits of a rectangular, planar  $\{\text{Fe}_4(\mu\text{-O})(\mu\text{-OH})(\text{hpdtA})_2(\text{H}_2\text{O})_4\}$  motif twist in respect to each other to give an overall tetrahedral arrangement of the  $\text{Fe}^{\text{III}}$  atoms. Furthermore, hydrated ferrous  $\text{Fe}^{\text{II}}$  centres can be utilised to link the rectangular tetranuclear  $\text{Fe}^{\text{III}}$  complexes to give nonanuclear mixed valent aggregates. These aggregation and core rearrangement processes are summarised in Fig. 1 and 2. We found that the direct combination of the dinuclear  $\{\text{Fe}_2(\text{hpdtA})\}$ -units leads to symmetric complexes where antiferromagnetic interactions stabilise  $S = 0$  spin ground states.<sup>7</sup> To synthesise less symmetrical complexes that give rise to uncompensated magnetic moments we applied, in consecutive experiments, two synthetic approaches. The first preparation method involves the use of an excess of metal salts so that  $\{\text{Fe}_2(\text{hpdtA})\}$ -units are able to encapsulate ionic groups or mineral fragments. One example of the successful outcome of this strategy is provided by the nonanuclear complex  $[\text{Fe}_9(\mu_3\text{-O})_4(\mu\text{-OH})_4(\text{hpdtA})_4]^{5-}$  in which an  $\text{Fe}^{\text{III}}$  centre is surrounded by four  $\{\text{Fe}_2(\text{hpdtA})\}$ -units.<sup>9</sup> When we investigated the corresponding Al/hpdtA system we found that analogous dinuclear subunits stabilise an Al<sub>7</sub>-boehmite-type mineral-fragment to give an  $[\text{Al}_{15}(\mu_3\text{-O})_4(\mu_3\text{-OH})_6(\mu\text{-OH})_{14}(\text{hpdtA})_4]^{2-}$  cluster (Fig. 2).<sup>10</sup>

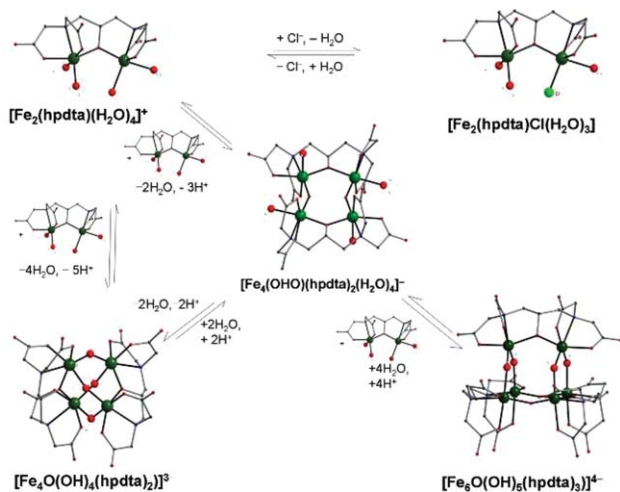


Fig. 1 Aggregation and core rearrangement reactions in the Fe(III)/hpdtA-system.<sup>7</sup>

Our second strategy uses an excess of organic bases or additional weaker complexing agents (co-ligands) that are capable of coordinating to the  $\text{Fe}^{\text{III}}$  centres thereby reducing the symmetry of the polynuclear aggregates. Such asymmetric iron coordination clusters can show interesting magnetic properties as a result of the variety of pairwise antiferromagnetic

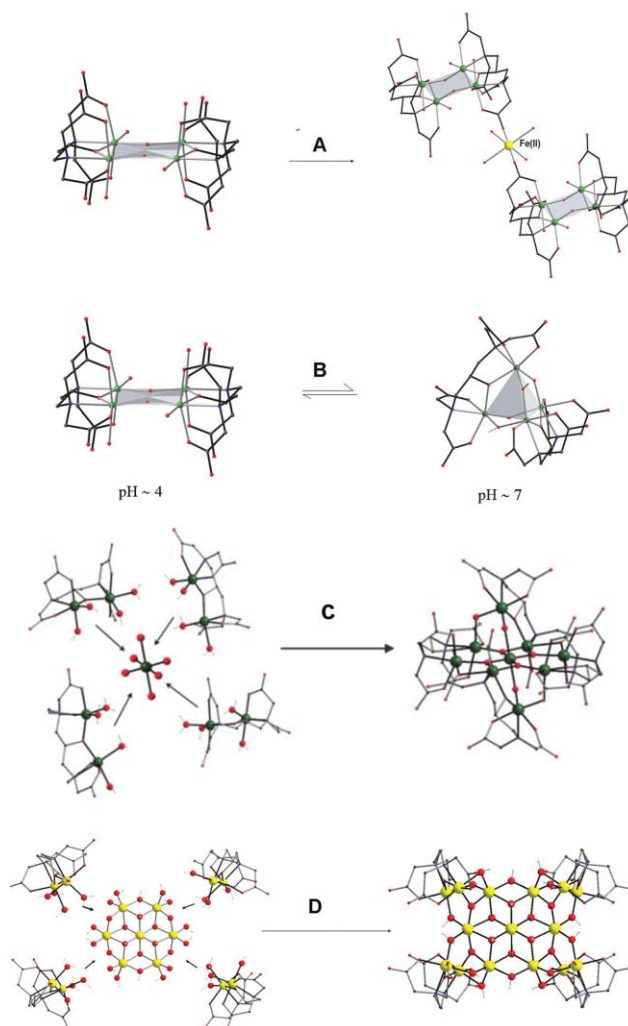
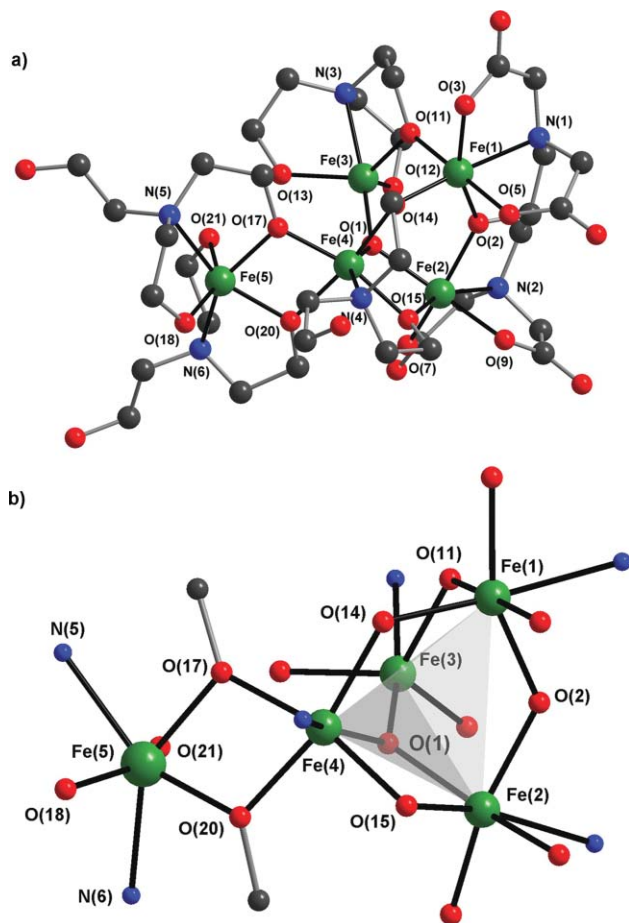


Fig. 2 (A) Linkage of  $\text{Fe}_4$  units through hydrated  $\text{Fe}^{\text{II}}$  ions; (B) core rearrangement of planar  $\text{Fe}_4$  complex into tetrahedral  $\text{Fe}_4$  structure;<sup>7</sup> Encapsulation of ionic groups or mineral fragments by dinuclear  $\text{M}_2(\text{hpdtA})$  units; (C) Formal hydrolytic encapsulation of  $[\text{Fe}(\text{H}_2\text{O})_6]^{3+}$  by four  $\{\text{Fe}_2(\text{hpdtA})(\text{H}_2\text{O})_4\}^+$  species to give  $[\text{Fe}_9(\mu_3\text{-O})_4(\mu\text{-OH})_4(\text{hpdtA})_4]^{5-}$ ;<sup>9</sup> (D)  $[\text{Al}_7(\text{OH})_{12}(\text{H}_2\text{O})_{12}]^{9+}$  by four  $\{\text{Al}_2(\text{hpdtA})(\text{H}_2\text{O})_4\}^+$ -units to give  $[\text{Al}_{15}(\mu_3\text{-O})_4(\mu_3\text{-OH})_6(\mu\text{-OH})_{14}(\text{hpdtA})_4]^{2-}$ .<sup>8,10</sup>

couplings leading to non-zero ground spin states even when there are even numbers of iron centres in the cluster.<sup>4b,i</sup> We report here the structures and the magnetic properties of a new penta- and a new nonanuclear  $\text{Fe}^{\text{III}}$ -oxo cluster  $[\text{Fe}_5(\mu_3\text{-O})(\text{hpdtA})(\text{H}_2\text{tea})(\text{Htea})_2(\text{tea})] \cdot \{\text{N}(\text{C}_2\text{H}_4\text{OH})_3\} \cdot 2\text{EtOH} \cdot 7\text{H}_2\text{O}$  (**1**) and  $[\text{Fe}_9(\mu_3\text{-O})_5(\mu\text{-OH})_5(\text{en})_6(\text{hpdtA})_2](\text{NO}_3)_2 \cdot 7\text{H}_2\text{O}$  (**2**) synthesised according to this second strategy.

## 2.2 The structure of $[\text{Fe}_5(\mu_3\text{-O})(\text{hpdt})_2(\text{H}_2\text{tea})(\text{Htea})_2(\text{tea})]\cdot\{\text{N}(\text{C}_2\text{H}_4\text{OH})_3\}_2\cdot 2\text{EtOH}\cdot 7\text{H}_2\text{O}$ (**1**)

$[\text{Fe}_5(\mu_3\text{-O})(\text{hpdt})_2(\text{H}_2\text{tea})(\text{Htea})_2(\text{tea})]\cdot\{\text{N}(\text{C}_2\text{H}_4\text{OH})_3\}_2\cdot 2\text{EtOH}\cdot 7\text{H}_2\text{O}$  (**1**) forms upon reaction of  $\text{FeCl}_3$ ,  $\text{H}_3\text{tea}$  and  $\text{H}_3\text{hpdt}$ . The compound crystallises in the triclinic space group  $P\bar{1}$  (No. 2). Fig. 3 illustrates the molecular structure of the  $\text{Fe}^{\text{III}}$  aggregate and shows the central Fe–O core in **1**. Within the pentanuclear coordination cluster the  $\text{Fe}^{\text{III}}$  centres are surrounded by one fully deprotonated  $\text{hpdt}^{5-}$  ligand and four triethanolamine ligands. Non-coordinating O-donors from the triethanolamine ligands remain protonated which results in the cluster containing one fully deprotonated  $\text{tea}^{3-}$  ligand, two mono protonated  $\text{Htea}^{2-}$  ligand and one doubly protonated  $\text{H}_2\text{tea}^-$  ligand. The  $\text{hpdt}^{5-}$  ligand binds to Fe(1) and Fe(2) forming the expected alkoxo bridged  $\{\text{Fe}_2(\text{hpdt})\}$ -unit<sup>7</sup> in which the carboxylate oxygen atoms and N-donors of the iminodiacetic acid moieties occupy *facial* positions of the distorted octahedral coordination spheres. Fe(1) and Fe(2) are additionally bonded *via* alkoxo groups of a  $\text{Htea}^{2-}$  ligand to Fe(4). Whilst the N-function of this ligand coordinates



**Fig. 3** a) The structure of  $[\text{Fe}_5(\mu_3\text{-O})(\text{hpdt})_2(\text{H}_2\text{tea})(\text{Htea})_2(\text{tea})]$  in **1**. H atoms are neglected for clarity; b) The Fe–O-core structure of **1**. Selected interatomic distances (Å) and -angles ( $^\circ$ ): Fe(1)–Fe(2) 3.494(2), Fe(1)–Fe(3) 3.437(1), Fe(1)–Fe(4) 3.479(2), Fe(2)–Fe(3) 3.433(2), Fe(2)–Fe(4) 3.021(1), Fe(3)–Fe(4) 3.412(2), Fe(4)–Fe(5) 3.157(2), Fe(3)–O(1) 1.863(6), Fe(2)–O(1) 2.024(5), Fe(4)–O(1) 1.936(5), Fe–O<sub>alkoxo</sub> 1.862(5)–2.027(6), Fe–N 2.216(6)–2.282(7), Fe(3)–O(1)–Fe(4) 127.9(3), Fe(3)–O(1)–Fe(2) 124.0(3), Fe(4)–O(1)–Fe(2) 99.44(2).

to Fe(4) the remaining alcohol group is not coordinated. The further five coordination sites of Fe(3) are occupied by the donors of an additional  $\text{Htea}^{2-}$  ligand that also links Fe(3) to Fe(1) through O(11). Fe(2), Fe(3) and Fe(4) form a  $\mu_3$ -oxo-centered  $\{\text{Fe}_3\text{O}\}$  unit for which the iron centres are far from equilateral but is near to planar with O(1) only 0.3243 Å out of the plane.

The arrangement of the transition metal ions Fe(1)–Fe(4) can best be described as distorted tetrahedron. The bonds Fe(2)–O(1), Fe(3)–O(1) and Fe(4)–O(1) are 2.024(5), 1.863(6) and 1.936(5) Å long, respectively; the Fe–Fe-distances within the tetrahedron vary between 3.021(1)–3.494(2) Å. As expected, the doubly-bridged iron atom pair Fe(2) and Fe(4) has the shortest interatomic distance. Fe(1) and Fe(2) in the  $\{\text{Fe}_2(\text{hpdt})\}$  unit reveal the largest Fe–Fe distance. *Cis* coordinating O donors from two different triethanolamine ligands bridge between Fe(4) and Fe(5) and their distorted octahedral coordination polyhedra share a common edge. The amine functions of these two triethanolamine ligands bind to Fe(5) and are at equatorial positions opposite to the common edge of the polyhedra. One O-donor of each of the triethanolamine ligands coordinates the apical position to Fe(5) while the other remaining alcohol functions remain uncoordinated. Fe(4) and Fe(5) reside 3.157(2) Å from each other. The distance between the two O-donors O(13) and O(21) of two triethanolamine ligands is 2.422(9) Å. The electron density in the Fourier-difference map between these two atoms was refined as a hydrogen atom which is consistent with the overall neutral charge of the cluster. The H atom binds to O(13) and points towards O(21) forming a strong intramolecular H-bond.

## 2.3 The structure of $[\text{Fe}_9(\mu_3\text{-O})_5(\mu\text{-OH})_5(\text{en})_6(\text{hpdt})_2](\text{NO}_3)_2\cdot \text{en}\cdot 7\text{H}_2\text{O}$ (**2**)

Diffusion of ethanol into methanol–water mixtures containing  $\text{Fe}^{\text{III}}(\text{NO}_3)_3\cdot 9\text{H}_2\text{O}$ , ethylenediamine and  $\text{H}_3\text{hpdt}$  results in the formation of crystals of  $[\text{Fe}_9(\mu_3\text{-O})_5(\mu\text{-OH})_5(\text{en})_6(\text{hpdt})_2](\text{NO}_3)_2\cdot 7\text{EtOH}$  (**2**). The compound crystallises in the triclinic space group  $P\bar{1}$  (No. 2), with two crystallographically independent oxo-clusters in the unit cell that exhibit minor structural differences. Fig. 4 illustrates one of the cluster cations, which will be subject of a more detailed structural discussion. Fig. 5 shows the Fe–O core.

Fe(1), situated in the centre of the nonanuclear  $\text{Fe}^{\text{III}}$  aggregate, is only five coordinate with a distorted trigonal-bipyramidal coordination environment of five  $\mu_3$ -oxo-ligands O(1)–O(5) each of which corresponds to the central oxygen of the asymmetric  $\{\text{Fe}_3\text{O}\}$  triangles. The geometry of the  $[\text{Fe}_9(\mu_3\text{-O})_5(\mu\text{-OH})_5(\text{en})_6(\text{hpdt})_2]^{2+}$  complexes shows small distortions from idealised  $C_2$ -symmetry with the two-fold axis running through Fe(1) and the hydroxo O-donors O(1) and O(6). Thus, in this idealised symmetry  $\{\text{Fe}_3\text{O}\}$ -fragments centred around O(2), O(3) and O(4), O(5) are related to each other, displaying similar distortions from an equilateral arrangement. Within the  $\{\text{Fe}_3\text{O}\}$ -segments the Fe–O-distances vary between 1.861(7)–2.032(6) Å, the interatomic Fe–Fe distances between 2.905(2)–3.536(2) Å.

Of particular note is the unusual T-shaped coordination environment of O(1) with an exceptionally large Fe(2)–O(1)–Fe(3) angle of 167.9(4) $^\circ$  combined with rather small Fe(1)–O(1)–Fe(2) and Fe(1)–O(1)–Fe(3) angles of 96.5(3) $^\circ$  and 95.4(3) $^\circ$ . The Fe–O–Fe angles in the other four triangles range from 94.8(3) $^\circ$  to

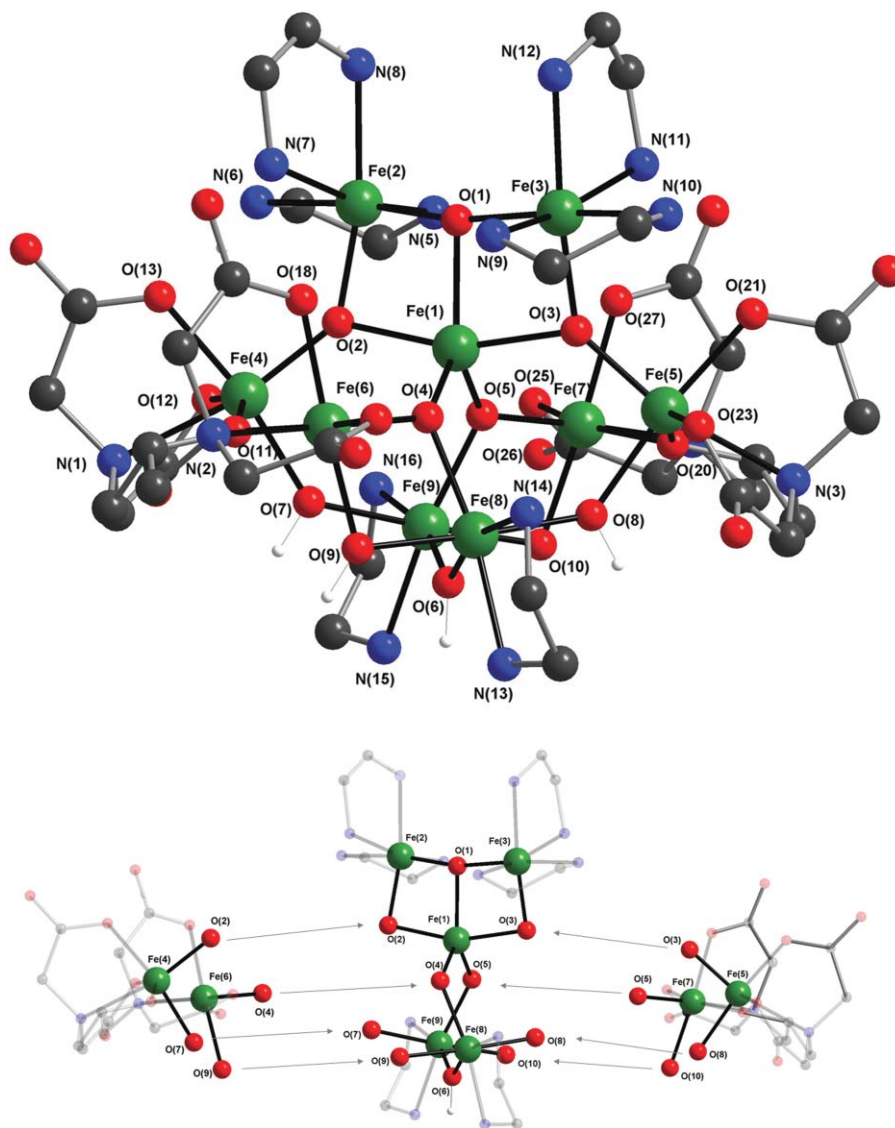


**Fig. 4** The structure of the  $[\text{Fe}_9(\mu_3\text{-O})_5(\mu\text{-OH})_5(\text{en})_6(\text{hpdta})_2]^{2+}$ -complex in **2** (top) and visualisation of the build-up of the oxo-cluster from dinuclear  $\{\text{Fe}_2(\text{hpdta})\}$  building units (bottom).

$139.0(4)^\circ$ . Fe(1) and Fe(2) are each further coordinated by two ethylenediamine ligands which bind with their N-donors in *cis* positions.

The ligand pairs O(2), O(4) and O(3), O(5) connect Fe(1) to two  $\{\text{Fe}_2(\text{hpdta})\}$  units in which the carboxylic O- and N-donors of the iminodiacetic acid moiety occupy *facial* positions of the distorted octahedral coordination spheres. In terms of the representation in Fig. 2 we can describe the  $\mu_3$ -oxo ligands O(2) and O(3) as binding upwards such that O(2) binds to Fe(2) and Fe(4), O(3) to Fe(3) and Fe(5). In this view O(4) and O(5) bind downwards to Fe(8) and Fe(9), respectively. Fe(8) and Fe(9) are hydroxo-bridged (*via* O(6)) and each Fe centre is coordinated by an ethylenediamine ligand with *via* N-donors in *cis* positions. The remaining *trans* positions of the distorted octahedral coordination polyhedra are occupied by further hydroxo ligands. O(8)/O(9) bind to Fe(8) and O(7)/O(10) bind to Fe(9) linking these Fe centres with the  $\{\text{Fe}_2(\text{hpdta})\}$ -units. The Fe–O<sub>hydroxo</sub> bond distances in **2** vary between 1.966(7)

Å and 2.018(7) Å; the angles Fe(7)–O(10)–Fe(9) and Fe(8)–O(9)–Fe(6) are with  $96.4(3)^\circ$  and  $96.7(3)^\circ$  significantly smaller than the Fe(4)–O(7)–Fe(9), Fe(8)–O(8)–Fe(5) and Fe(8)–O(6)–Fe(9) angles which are  $133.3(3)^\circ$ ,  $133.4(4)^\circ$  and  $130.9(3)^\circ$ , respectively. The bond distances of the Fe<sup>III</sup> ions to N-donors of the ethylenediamine ligands vary between 2.118(8) and 2.283(8) Å.

#### The magnetic properties of $[\text{Fe}_5(\mu_3\text{-O})(\text{hpdta})(\text{H}_2\text{tea})(\text{Htea})_2(\text{tea})]\cdot\{\text{N}(\text{C}_2\text{H}_4\text{OH})_3\}\cdot 2\text{EtOH}\cdot 7\text{H}_2\text{O}$ (**1**) and $[\text{Fe}_9(\mu_3\text{-O})_5(\mu\text{-OH})_5(\text{en})_6(\text{hpdta})_2](\text{NO}_3)_2\cdot 7\text{H}_2\text{O}$ (**2**)

The temperature dependence of the magnetic susceptibility of **1** was measured between 298 and 2 K (Fig. 6a). The  $\chi T$ -value of 8.35 emu K mol<sup>-1</sup> at room temperature is significantly lower than that expected for five uncoupled Fe<sup>III</sup> high spin ions (21.875 emu mol<sup>-1</sup> K with  $g = 2.0$ ). The presence of antiferromagnetic interactions is confirmed by the nearly linear decrease of the  $\chi T$  product.

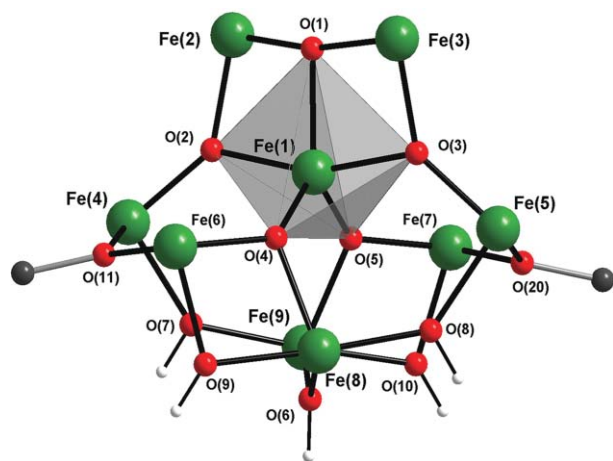


Fig. 5 The Fe–O core in  $[\text{Fe}_9(\mu_3\text{-O})_5(\mu\text{-OH})_5(\text{en})_6(\text{hpdta})_2]^{2+}$ .

The measurement at 0.1 T reaches a minimum of  $4.15 \text{ emu mol}^{-1} \text{ K}$  (30–25 K), followed by a rapid increase up to  $5.50 \text{ emu mol}^{-1} \text{ K}$  (2 K).

The  $\chi T$  data points recorded at a higher magnetic field (1 T) lie at lower temperatures slightly above the values measured at 0.1 T. They reach a minimum of  $4.15 \text{ emu mol}^{-1} \text{ K}$  at 36 K. Below this temperature the graph increases again to  $4.62 \text{ emu mol}^{-1} \text{ K}$  at 5 K followed by a rapid decrease to  $3.77 \text{ emu mol}^{-1} \text{ K}$  (2 K). The Curie constant of a system with a spin ground state of  $S = 5/2$  and  $g = 2$  is expected to be  $C = Ng^2\mu_B^2/3k_B S(S+1) = 4.38 \text{ emu K mol}^{-1}$ . Fig. 2b illustrates the field dependence of the magnetisation of **1** measured at 1.8 K. Saturation effects are observed, as indicated by the  $\chi T$  vs.  $T$  graph, at a magnetic field of *ca.* 1 T. A saturation value of  $26300 \text{ emu}^{-1} \text{ mol}$  (see inset of Fig. 6a) is in good agreement with an  $S = 5/2$  ground state.

Crystals of **2** start to lose solvent immediately on isolation from the mother liquor. In agreement with results of the elemental analysis the composition of the examined sample is best represented by the formula  $[\text{Fe}_9(\mu_3\text{-O})_5(\mu\text{-OH})_5(\text{en})_6(\text{hpdta})_2(\text{NO}_3)_2 \cdot 7\text{H}_2\text{O}$  (**2**). The IR spectrum of this substance confirms that the integrity of the nonanuclear cluster is retained even after partial solvent loss.

Fig. 6b shows the temperature dependence of  $\chi T$  of **2** which is qualitatively very similar to that of **1**. The value of  $\chi T$  at room temperature is *ca.*  $13.5 \text{ emu mol}^{-1} \text{ K}$ , well below that expected for nine non-interacting  $S = 5/2$  centres with  $g = 2$  (which is  $39.375 \text{ emu}$

$\text{mol}^{-1} \text{ K}$ ) and indicative of pairwise antiferromagnetic interactions giving rise to an uncompensated moment. The presence of antiferromagnetic interactions is further substantiated by the fact that the  $\chi T$  product decreases on lowering the temperature to reach a minimum of  $10.2 \text{ emu mol}^{-1} \text{ K}$  between 55 and 40 K. This is followed by a rapid increase up to a maximum of  $11.5 \text{ emu mol}^{-1} \text{ K}$  at 4 K in a field of 0.1 T. At a higher magnetic field (1 T) the graph exhibits a maximum at a slightly lower value of  $10.7 \text{ emu mol}^{-1} \text{ K}$  followed by a rapid decrease to  $6.02 \text{ emu mol}^{-1}$ . This slightly different behaviour is due to field induced saturation effect. The expected Curie constant of a system with a  $S = 7/2$  spin ground state (with  $g = 2$ ) is  $7.9 \text{ emu K mol}^{-1}$ , of a compound with an  $S = 9/2$  state  $12.3 \text{ emu K mol}^{-1}$ .

Fig. 6b (*inset*) shows the field dependence of the magnetisation revealing a rapid increase of the slope and first saturation effects below 1 T. The coordination compound reaches a saturation of the magnetisation of *ca.*  $39150 \text{ emu mol}^{-1}$  at 7 T which is close to the expected saturation of a spin ground state of  $S = 7/2$  (with  $g = 2$ ).

### 3 Summary

We have reported the synthesis and structures of two new polynuclear iron(III) oxo clusters. These two complexes with unprecedented Fe–O core structures extend our knowledge of the *hpdta* reaction system and help us to develop a synthetic concept to rationalise the build-up of structures with properties of potential molecular magnets. Our basic synthetic methodology takes advantage of  $\{\text{Fe}_2\text{hpdta}(\text{H}_2\text{O})_4\}$  sub-units that form *in situ* in solution or that can be isolated as neutral  $[\text{Fe}_2\text{hpdta}(\text{Cl})(\text{H}_2\text{O})_3]$  complexes.<sup>7</sup> Our experiments indicate that these subunits aggregate through condensation reactions forming larger coordination clusters. Additional tripod ligands (*e.g.*  $\text{H}_3\text{tea}$ ) or organic bases which also bind to the  $\text{Fe}^{\text{III}}$  centres allow for the formation of less symmetrical clusters compared with the previously reported polynuclear complexes where we combined the dinuclear  $\{\text{Fe}_2\text{hpdta}(\text{H}_2\text{O})_4\}$  building units directly. Preliminary studies on the magnetic properties revealed that the clusters represent molecular ferrimagnetic systems where uncompensated antiferromagnetic interactions lead to  $S \neq 0$  ground states. We are currently investigating how the  $\{\text{Fe}_2\text{hpdta}(\text{H}_2\text{O})_4\}$  subunits can be used to encapsulate larger mineral fragments present in aqueous solutions.

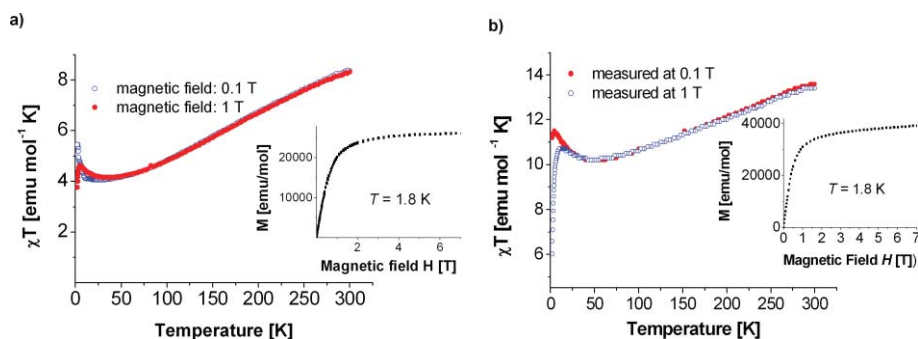


Fig. 6 a) The magnetic properties of **1**.  $\chi T$  vs.  $T$  and field dependence of the magnetisation (*inset*). b) The magnetic properties of **2**.  $\chi T$  vs.  $T$  and the field dependence of the magnetisation (*inset*).

## 4 Experimental

All reagents were used as received from Aldrich Chemicals. Magnetic measurements were performed on a Quantum Design SQUID magnetometer on polycrystalline samples. Data were corrected for diamagnetism of the sample and holder. IR-spectra were recorded using a Perkin-Elmer "Spectrum One" Fourier transform infrared (FTIR) spectrometer. Samples were prepared as KBr disks. X-ray crystallography for **1** and **2** (Table 1): Data were collected at 200 K on Bruker SMART Apex (**1**) and STOE IPDS (**2**) diffractometers with graphite-monochromated Mo-K $\alpha$  radiation. Structures were solved by direct methods and refined by full-matrix in a least-squares refinement on  $F$ , using the SHELX-TL software suite.<sup>11</sup> **2** contains a large number of highly disordered solvent molecules and we applied the programme SQUEEZE to account for the disordered solvent molecules.<sup>12</sup> We successfully located 7 constitution water molecules per oxo-cluster; the as-prepared crystals are expected to contain additional solvent molecules. The formula  $[\text{Fe}_9(\mu_3\text{-O})_5(\mu\text{-OH})_5(\text{en})_6(\text{hpdt})_2](\text{NO}_3)_2 \cdot 7\text{H}_2\text{O}$  (**2**) is in good agreement with the elemental analysis of a sample stored at room temperature. Crystallographic data (excluding structure factors) have been deposited with the Cambridge Crystallographic Data Centre with CCDC reference numbers 781103 (**1**) and 781104 (**2**).<sup>†</sup> Copies of the data can be obtained, free of charge, on application to CCDC, 12 Union Road, Cambridge CB2 1EZ, UK (fax: 1 44-1223-336-033 or e-mail: deposit@ccdc.cam.ac.uk).

### Synthesis of $[\text{Fe}_5(\mu_3\text{-O})(\text{hpdt})_2(\text{H}_2\text{tea})(\text{Htea})_2](\text{tea}) \cdot \{\text{N}(\text{C}_2\text{H}_4\text{OH})_3\} \cdot 2\text{EtOH} \cdot 7\text{H}_2\text{O}$ (**1**)

To prepare complex **1**, 0.040 g (0.125 mmol)  $H_5\text{hpdt}$  were dissolved in 5 ml methanol by addition of 0.3 ml triethanolamine. The complexing agents were added to a stirred solution of 10 ml  $\text{FeCl}_3/\text{methanol}$  (0.15 M) and left for slow evaporation of the solvent. After half of the solvent was evaporated, slow diffusion of EtOH into the reaction mixture led to the crystallisation of orange plates within three weeks. Yield: 0.061 g (31% based on  $H_5\text{hpdt}$ ). Elemental analysis calculated for  $\text{C}_{45}\text{Fe}_5\text{H}_{106}\text{N}_7\text{O}_{34}$ : C 34.46%, H 6.81%, N 6.25%, found: C 34.12%, H 6.51%, N 6.42%. IR-data ( $\text{cm}^{-1}$ ): 3355 (st), 2871 (m), 1634 (vst), 1459 (m), 1385 (st), 1270 (m), 1068 (st), 916 (m), 900 (m), 737 (m), 616 (m).

### Synthesis of $[\text{Fe}_9(\mu_3\text{-O})_5(\mu\text{-OH})_5(\text{en})_6(\text{hpdt})_2](\text{NO}_3)_2 \cdot 7\text{H}_2\text{O}$ (**2**)

To prepare complex **2**, 0.040 g (0.125 mmol)  $H_5\text{hpdt}$  were dissolved in 5 ml methanol by addition of 0.2 ml ethylenediamine. The complexing agents were added to a stirred solution of 0.303 g (0.75 mmol)  $\text{Fe}(\text{NO}_3)_3 \cdot 9\text{H}_2\text{O}$  in 5 ml methanol. Slow diffusion of EtOH into the reaction mixture led to the crystallisation of dark red crystals of **2** within two weeks. Yield: 0.043 g (30% based on  $H_5\text{hpdt}$ ). Elemental analysis calculated for  $\text{C}_{34}\text{H}_{93}\text{Fe}_9\text{N}_{18}\text{O}_{41}$ , which corresponds to the crystallographically determined formulation with the loss of one ethylenediamine molecule, 6.5 ethanol- and 1.5 water molecules: C 21.35%, H 4.90%, N 13.18%; found C: 20.21%, H: 5.15%, N 13.54%. IR-Data ( $\text{cm}^{-1}$ ): 3421 (st), 3313 (st, br), 2948 (m), 1629 (vst), 1384 (vst), 1170 (w), 1105 (w, br), 1040 (m), 975 (w), 909 (m), 735 (m), 689 (m), 630 (st), 532 (m).

**Table 1** Crystal data and structure refinements for compounds **1** and **2**

	1	2
Formula	$\text{C}_{45}\text{H}_{106}\text{Fe}_5\text{N}_7\text{O}_{34}$	$\text{C}_{68}\text{H}_{186}\text{Fe}_{18}\text{N}_{36}\text{O}_{82}$
fw	1568.62	3643.28
$T/\text{K}$	200(2)	200(2)
Cryst. syst.	Triclinic	Triclinic
Space group	$P\bar{1}$	$P\bar{1}$
$a/\text{\AA}$	12.8196(9)	17.0895(13)
$b/\text{\AA}$	15.1458(10)	23.847(2)
$c/\text{\AA}$	18.8635(13)	24.049(2)
$\alpha$ ( $^\circ$ )	75.873(8)	64.4540(10)
$\beta$ ( $^\circ$ )	70.197(8)	81.699(2)
$\gamma$ ( $^\circ$ )	78.956(8)	87.770(2)
$V/\text{\AA}^3$	3317.9(4)	8746.9(12)
$Z$	2	2
$D_c/\text{g cm}^{-3}$	1.546	1.383
$\mu/\text{mm}^{-1}$	1.161	1.528
GOF	1.016	0.974
$R_1^a$ ( $I > 2\sigma(I)$ )	0.0681	0.0794
$wR_2^a$ (all data)	0.1775	0.2405

<sup>a</sup>  $R_1 = \sum \|F_o\| - |F_c|/\sum \|F_o\|$ ;  $wR_2 = \{\sum [w(F_o^2 - F_c^2)^2]/\sum [w(F_o^2)^2]\}^{1/2}$ ,  $w = 1/[\sigma^2(F_o^2) + (aP)^2 + bP]$ , where  $P = [\max(F_o^2, 0) + 2F_c^2]/3$  for all data.

## Acknowledgements

This work was supported by the DFG Center for Functional Nanostructures (CFN) and the EU-FP6 RTN QUEMOLNA and NOE MAGMANET. The authors are grateful for the support through the Science Foundation Ireland (08/IN.1/I2047 and 08/RFP/CHE1273). L. Z. thanks IRCSET for a postdoctoral fellowship.

## Notes and references

- (a) R. Laye and E. J. L. McInnes, *Eur. J. Inorg. Chem.*, 2004, 2811; (b) R. E. P. Winpenny, *Adv. Inorg. Chem.*, 2001, **52**, 1; (c) C. J. Milios, S. Piligkos and E. K. Brechin, *Dalton Trans.*, 2008, 1809; (d) G. E. Kostakis, I. J. Hewitt, A. M. Ako, V. Mereacre and A. K. Powell, *Phil. Trans. R. Soc. A*, 2010, **368**, 1509.
- (a) D. Gatteschi and R. Sessoli, *Angew. Chem. Int. Ed. Engl.*, 2003, **42**, 268 and refs therein; (b) G. A. Timco, S. Carretta, F. Troiani, F. Tuna, R. J. Pritchard, C. A. Muryn, E. J. L. McInnes, A. Ghirri, A. Candini, P. Santini, G. Amoretti, M. Affronte and R. E. P. Winpenny, *Nature Nanotech.*, 2009, **4**, 173; (c) M. Leuenberger and D. Loss, *Nature*, 2001, **410**, 789; (d) N. Baadji, M. Piacenza, T. Tugsuz, F. Della Sala, G. Maruccio and S. Sanvito, *Nature Mat.*, 2009, **9**, 813.
- R. M. Cornell and U. Schwertmann, *The Iron Oxides*, 2nd Ed. 2002, Wiley-VCH, Weinheim.
- Selected examples of Fe-oxo-clusters*: (a) K. Wieghardt, K. Pohl, I. Jibril and G. Huttner, *Angew. Chem. Int. Ed. Engl.*, 1984, **23**, 77; (b) W. Schmitt, C. E. Anson, R. Sessoli, M. Van Veen and A. K. Powell, *J. Inorg. Biochem.*, 2002, **91**, 173; (c) S. M. Gorun, G. C. Papaefthymiou, R. B. Frankel and S. J. Lippard, *J. Am. Chem. Soc.*, 1987, **109**, 3337; (d) K. L. Taft and S. J. Lippard, *J. Am. Chem. Soc.*, 1990, **112**, 9629; (e) A. M. Ako, O. Waldmann, V. Mereacre, F. Klöwer, I. J. Hewitt, C. E. Anson, H. U. Güdel and A. K. Powell, *Inorg. Chem.*, 2007, **46**, 756; (f) S. P. Watton, P. Fuhrmann, L. E. Pence, A. Caneschi, A. Cornia, G. L. Abbati and S. J. Lippard, *Angew. Chem.*, 1997, **109**, 2917; S. P. Watton, P. Fuhrmann, L. E. Pence, A. Caneschi, A. Cornia, G. L. Abbati and S. J. Lippard, *Angew. Chem. Int. Ed. Engl.*, 1997, **36**, 2774; (g) K. L. Taft, G. C. Papaefthymiou and S. J. Lippard, *Inorg. Chem.*, 1994, **33**, 1510; (h) A. M. Ako, V. Mereacre, Y. Lan, W. Wernsdorfer, R. Clérac, C. E. Anson and A. K. Powell, *Inorg. Chem.*, 2010, **49**, 1; (i) A. Caneschi, A. Cornia, A. C. Fabretti and D. Gatteschi, *Angew. Chem. Int. Ed. Engl.*, 1995, **34**, 2716; (j) W. Micklitz and S. J. Lippard, *J. Am. Chem. Soc.*, 1989, **111**, 6856; (k) G. C. Papaefthymiou, *Phys. Rev. B*, 1992, **46**, 10366; (l) C. J. Harding, R. K. Henderson and A. K. Powell, *Angew. Chem. Int. Ed. Engl.*, 1993, **32**, 570; (m) K. S. Hagen

- and V. S. Nair, *Inorg. Chem.*, 1994, **33**, 185; (n) K. Hegetschweiler, H. W. Schmalle, H. M. Streit, V. Gramlich, H.-U. Hund and I. Erni, *Inorg. Chem.*, 1992, **31**, 1299; (o) S. Konar and A. Clearfield, *Inorg. Chem.*, 2008, **47**, 5573; (p) L. F. Jones, P. Jensen, B. Moubaraki, K. J. Berry, J. F. Boas, J. R. Pilbrow and Keith S. Murray, *J. Mater. Chem.*, 2006, **16**, 2690; (q) L. F. Jones, E. K. Brechin, D. Collison, M. Helliwell, T. Mallah, S. Piligkos, G. Rajaraman and W. Wernsdorfer, *Inorg. Chem.*, 2003, **42**, 6601; (r) S. Konar and A. Clearfield, *Inorg. Chem.*, 2008, **47**, 5573; (s) S. Konar, N. Bhuvanesh and A. Clearfield, *J. Am. Chem. Soc.*, 2006, **128**, 9604; (t) M. Murugesu, R. Clérac, W. Wernsdorfer, C. E. Anson and A. K. Powell, *Angew. Chem. Int. Ed.*, 2005, **44**, 6678; (u) K. L. Taft, C. D. Delfs, G. C. Papaefthymiou, S. Foner, D. Gatteschi and S. J. Lippard, *J. Am. Chem. Soc.*, 1994, **116**, 823; (v) N. Hoshino, A. M. Ako, A. K. Powell and H. Oshio, *Inorg. Chem.*, 2009, **48**, 2296; (w) K. L. Taft, G. C. Papaefthymiou and S. J. Lippard, *Science*, 1993, **259**, 1302.
- 5 (a) W. Wernsdorfer, R. Sessoli, A. Caneschi, D. Gatteschi and A. Cornia, *Europhys. Lett.*, 2000, **50**, 552; (b) W. Wernsdorfer, R. Sessoli, A. Caneschi, D. Gatteschi, A. Cornia and D. Mailly, *J. Appl. Phys.*, 2000, **87**, 5481; (c) D. Gatteschi, R. Sessoli and A. Cornia, *Chem. Commun.*, 2000, 725; W. Wernsdorfer and R. Sessoli, *Science*, 1999, **284**, 133; (d) Evangelisti A. Candini, M. Affronte, E. Pasca, L. J. de Jongh, R. T. W. Scott and E. K. Brechin, *Phys. Rev. B.*, 2009, **79**, 104414.
- 6 (a) A. Sigel, H. Sigel (eds), *Metal Ions in Biological Systems*, Vol. 35, Marcel Dekker Inc., New York, 1998; (b) R. R. Crichton in *Inorganic Biochemistry of Iron Metabolism*, Horwood, New York 1991; (c) M. Costas, M. P. Mehn, M. P. Jensen and L. Que, *Chem. Rev.*, 2004, **104**, 939; (d) E. Y. Tshuva and S. J. Lippard, *Chem. Rev.*, 2004, **104**, 987; (e) J. U. Rohde, J. H. In, M. H. Lim, W. W. Brennessel, M. R. Bukowski, A. Stubna, E. Muenck, W. Nam and L. Que Jr, *Science*, 2003, **299**, 1037.
- 7 W. Schmitt, C. E. Anson, B. Pilawa and A. K. Powell, *Z. anorg. allg. Chem.*, 2002, **628**, 2443.
- 8 (a) A. K. Powell, S. L. Heath, D. Gatteschi, L. Pardi, R. Sessoli, G. Spina, F. Del Giallo and F. Pieralli, *J. Am. Chem. Soc.*, 1995, **117**, 2491; (b) W. Schmitt, P. Hill, M. P. Juanico, A. Caneschi, F. Costantino, C. E. Anson and A. K. Powell, *Angew. Chem. Int. Ed.*, 2005, **44**, 4187; (c) W. Schmitt, J. P. Hill, S. Malik, C. Volkert, I. Ichinose, C. E. Anson and A. K. Powell, *Angew. Chem. Int. Ed.*, 2005, **44**, 7048; (d) I. McKeogh, J. P. Hill, E. S. Collins, T. McCabe, A. K. Powell and W. Schmitt, *New J. Chem.*, 2007, **31**, 1882; (e) W. Schmitt, P. A. Jordan, R. K. Henderson, G. R. Moore, C. E. Anson and A. K. Powell, *Coord. Chem. Rev.*, 2002, **228**, 115.
- 9 W. Schmitt, C. E. Anson, W. Wernsdorfer and A. K. Powell, *Chem. Commun.*, 2005, 2098.
- 10 W. Schmitt, E. Baissa, A. Mandel, C. E. Anson and A. K. Powell, *Angew. Chem. Int. Ed. Eng.*, 2001, **40**, 3577.
- 11 G. M. Sheldrick, *SHELXTL-NT*, 5.1, Bruker Analytical X-ray Systems, Madison, WI, 1997.
- 12 A. L. Spek, *J. Appl. Cryst.*, 2003, **36**, 7.